DOI: 10.1021/ma102196q

Macromolecules
ARTICLE

Self-Assembly and Micellization of a Dual Thermoresponsive Supramolecular Pseudo-Block Copolymer

Zhong-Xing Zhang,[†,‡] Kerh Li Liu,[‡] and Jun Li*[,†,‡]

[†]*Division of Bioengineering, Faculty of Engineering, National University of Singapore, 7 Engineering Drive 1, Singapore 117574, and* [‡]*Institute of Materials Research and Engineering, A*STAR (Agency for Science, Technology and Research), 3 Research Link, Singapore 117602, Republic of Singapore*

Received September 22, 2010; Revised Manuscript Received January 5, 2011

ABSTRACT: This paper reports the studies on self-assembly and thermosensitive micellization phenomena of a supramolecular polymeric host−guest system consisting of star-shaped poly(*N*-isopropylacrylamide) (PNIPAAm) with a β-cyclodextrin (β-CD) core (the host polymer) and bis(adamantyl)-terminated poly(propylene glycol) (PPG) (the guest polymer) in aqueous solution. This interesting host−guest system exhibited dual thermoresponse in aqueous solution because of the existence of two kinds of thermoresponsive segments, PPG and PNIPAAm, in the polymeric guest and host components, respectively. This unique thermoresponsive behavior was completely tunable by the ratio of host/guest up to 1.0. Beyond this range, the effect of the host was saturated, indicating that the host−guest system involved a 1:1 complexation between adamantyl moiety and β-CD core. In other words, this polymeric host−guest system was able to form ABA-type supramolecular pseudo-block copolymer via inclusion complexation in aqueous solution. This pseudo-block copolymer underwent a reversible temperature-induced transition from solution to micelle and further to aggregate under suitable conditions. However, different from conventional polymeric micelles, in the micelles formed from this pseudo-block copolymer, the shell (composed of host component) and the core (composed of guest component) were connected by physical interactions rather than chemical bonding. The micellization phenomena of the host−guest system were extensively studied by a combination of ^{1}H NMR, fluorescence probe technique, dynamic light scattering (DLS), transmission electron microscopy (TEM), and atomic force microscopy (AFM). The critical micelle temperature (CMT) for this thermoresponsive host−guest system was dependent on the composition and concentration of the components. The size of the resultant noncovalently connected micelle could be easily tuned not only by adjusting the temperature and the concentration of the components but also by the ratio of host/guest and the length of the PPG block in the guest polymer.

1. Introduction

Conventional amphiphilic di- or triblock copolymers can self-assemble to form nanostructures such as micelles in aqueous medium, containing dense cores of the insoluble blocks, surrounded by diffuse outer shells (coronas) formed by the soluble blocks. These polymeric micelles may have promising biomedical applications in drug and gene delivery, protein encapsulation, and so on.[1−3]

Recently, construction of micelles by using the nonconventional method is arousing people's interest.[4,5] Different from conventional polymeric micelles, in these micelles, which can be called as "noncovalently connected micelles (NCCMs)", only physical interactions rather than chemical bonds exist between shell and core. To construct such micelles, hydrophilic component A and hydrophobic component B are usually needed, which can interact with each other via H-bonding,[4,5] host−guest inclusion complexation,[6,7] and ligand−metal coordination interactions[8] in aqueous solution. The micelle formation in the aqueous mixture of A and B is usually induced by means of intrinsic hydrophobic interactions between chains of component B or external stimuli such as temperature, pH, and UV/vis light irradiation, etc. To date, NCCMs constructed with other noncovalent interactions except H-bonding as driving force are relatively seldom reported.

*Corresponding author: e-mail bielj@nus.edu.sg; Tel +65-6516-7273; Fax +65-6872-3069.

It was well-known that cyclodextrins (CDs) are a series of natural cyclic oligosaccharides composed of 6, 7, or 8 D-(+)-glucose units linked by α-1,4-linkages and named α-, β-, or γ-CD, respectively.[9] Because of their unique capability of forming inclusion complexes in the inner cavities and many other favorable physicochemical and biological properties, natural CDs and their derivatives have been recognized as important natural host molecules in the field of supramolecular chemistry.[10−16] Investigations by us and others in recent years have shown that the CD-based inclusion complexes have many promising applications, particularly in the areas of biotechnology and biomedicine.[17−19] Recently, we demonstrated a novel supramolecular approach controlling the thermoresponsive property of a poly(*N*-isopropylacrylamide) (PNIPAAm) star polymer through inclusion complexation between β-CD moiety and adamantyl groups.[20] PNIPAAm is one of the most popular thermoresponsive polymers, which shows dramatic and reversible phase transition behavior in water with the lower critical solution temperature (LCST) at 32 °C.[21] This unique property makes PNIPAAm and its copolymers "intelligent" systems for many promising applications, particularly in the areas of biotechnology, biomedicine, and nanotechnology, e.g., for controlled drug delivery, gene delivery, cell and enzyme immobilization, biosensor, and bioaffinity separation.[22−33]

Herein, we presented a design of a dual thermoresponsive supramolecular pseudo-block copolymer and its formation of

 Published on Web 02/04/2011

Scheme 1. Synthetic Procedures for (a) the β-CD-Based Macroinitiator (4Br-β-CD) and β-CD-Core Star-Shaped PNIPAAm (β-CD-(PNIPAAm)$_4$) via ATRP (Both Have an Average Degree of Substitution of 4) and (b) the Adamantyl-Containing PPGs

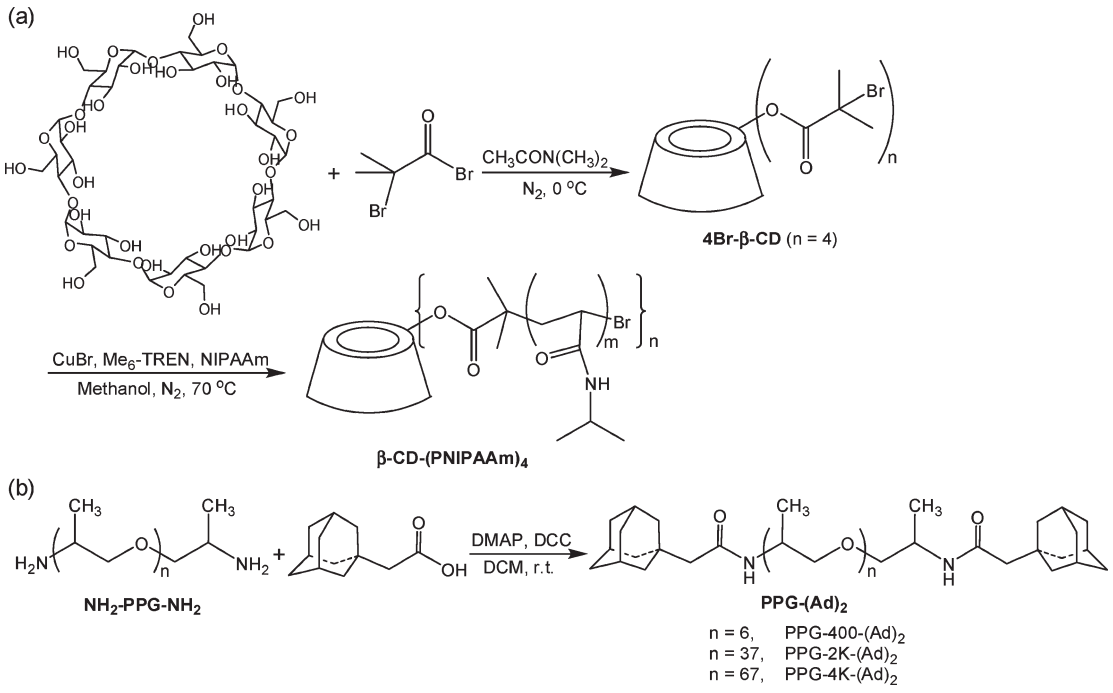

noncovalently connected micelles with PNIPAAm-grafted β-CD as the shell and poly(propylene glycol) (PPG) as the core. The supramolecular pseudo-block copolymer was formed from a polymeric host−guest pair, i.e., star-shaped PNIPAAm with a β-CD core (host polymer) and bis(adamantyl)-ended PPG (guest polymer) via host−guest inclusion complexation in aqueous solution. Upon the host−guest complexation, the resultant pseudo-block copolymer exhibited interesting dual thermoresponse in aqueous solution because of the existence of two kinds of thermoresponsive segments, PPG and PNIPAAm, in polymeric guest and host components, respectively, and this unique thermoresponsive behavior was completely tunable by the ratio of host/guest.

This pseudo-block copolymer showed thermosensitive micelle formation behavior in aqueous solution. That is, under lower temperature, the PPG chain of the guest polymer kept water-soluble, and no micelle was formed. As temperature increased, the PPG chains dehydrated and aggregated through hydrophobic−hydrophobic interactions, thus acting as a hydrophobic core for the micelle formation. When temperature further increased, the phase transition related to PNIPAAm on the corona of the noncovalently connected micelles occurred. Thus, the micelles were destabilized, resulting in micelle aggregation and precipitation. This solution−micellization−micelle destabilization process was totally temperature-reversible. The supramolecular system presented here is very different from the reported systems,[6,7] in the system components design, the tunability to respond to stimuli, the mechanism of noncovalently connected micelle formation, and the structure of the resultant micelles. Through forming the dual thermoresponsive pseudo-block copolymer, this work has demonstrated a novel supramolecular approach in designing and constructing noncovalently connected polymeric micelles with tunable properties.

2. Results and Discussion

2.1. Synthesis and Characterization of Host and Guest Polymers. *2.1.1. Star-Shaped PNIPAAm with a β-CD Core (Host Polymer).* This macromolecular host was synthesized using copper(I)-mediated ATRP according to our previous report,[20] which was featured with a β-CD core as a molecular recognition moiety and multiple PNIPAAm arms as actuation moieties. Scheme 1a shows the synthetic route of star-shaped PNIPAAm. First, a β-CD-based macroinitiator (4Br-β-CD) was synthesized by treating native β-CD with 4 equiv of 2-bromoisobutyric bromide. In our experimental conditions, the introduction of the initiation group, −OCO−C(CH$_3$)$_2$Br, to β-CD ring via esterification reaction occurred mainly at the 6-positioned primary hydroxyl group of the β-CD ring. In other words, the initiation groups were mainly grafted onto the smaller rim of the β-CD ring in the macroinitiator, which was confirmed by ^{13}C NMR analysis of the macroinitiator. A method for purifying this macroinitiator was based on the difference in solubility of initiator-modified β-CDs with different degree of substitution (DS) in water and acetone (DS is defined as the number of grafted initiation group per CD molecule). It was found that the solubility of these β-CD based macroinitiators in H_2O decreased dramatically with increasing DS. By contrast, their solubility in acetone increased distinctly with the increase of DS. Among them, the β-CD-based macroinitiator with DS of 4, was slightly soluble in both water and acetone. Thus, washing the crude product with water removed the macroinitiators with DS < 4, while washing the crude product with acetone removed the macroinitiators with DS > 4. By using this purification method, the β-CD-based macroinitiator with DS of 4 could be ensured a high level of purity. The DS of the purified macroinitiator was determined by means of ^{1}H NMR spectroscopy (DS ca. 3.9) and X-ray photoelectron spectroscopy (XPS) (DS ca. 4.3), respectively. Both methods indicated that the DS was very close to 4.

Second, ATRP of NIPAAm using 4Br-β-CD as macroinitiator was carried out under a nitrogen environment in the presence of copper(I) bromide as catalyst and Me$_6$-TREN as ligand. Referenced to literature methods of ATRP,[34,35] various experimental conditions were tested in order to synthesize well-defined star polymers. It was found that the best result could be obtained when methanol was chosen as reaction medium to give a homogeneous reaction system, the

initial molar ratio of [monomer]/[initiation site]/[CuBr]/[Me_6-TREN] ($[M]_0/[I]_0/[Cu]_0/[L]_0$) was 30/1/1/1.2, and the reaction temperature was at 70 °C. During the ATRP of NIPAAm in methanol using 4Br-β-CD as initiator, the monomer conversion was controlled to be less than 50% to limit possible side reactions such as bimolecular termination or thermal initiation. The number-average molecular weight (M_n) of the final star polymer calculated based on ^{1}H NMR, XPS, and GPC measurements was 8166, 9169, and 4101 Da (M_w/M_n = 1.24), respectively. These values based on different measurements were found to correlate well with the predicted molecular weight (7851 Da) calculated from the feed initiator concentration and the consumption of monomer, showing that the above-mentioned side reactions were negligible under our polymerization conditions.[20]

2.1.2. Bis(adamantyl)-Terminated PPGs (Guest Polymers). Theses macromolecular guests were obtained in high yield by mixing the corresponding bis(amino)-ended PPGs with adamantaneacetic acid in the presence of DCC and DMAP (Scheme 1b). The bifunctional PPGs were attached with adamantyl groups quantitatively. The attachment of two adamantyl groups to PPGs was confirmed by comparing the integral intensities of the peaks from the PPG segments (1.00−1.20 ppm) and the adamantyl groups (1.85−2.05 ppm) on their ^{1}H NMR spectra ($CDCl_3$). After modification of these PPGs with adamantaneacetic acid, a slight increase in molecular weight was observed by using GPC technique.

To further confirm the end-functionality of these adamantyl-containing PPGs, a derivatization strategy was employed to simplify the analysis of the polymer end group by NMR. Herein the trichloroacetyl isocyanate (TCAI) was used as derivatization reagent. TCAI was known to react quantitatively with amino groups, which causes a significant downfield shift of the initial protons adjacent to these amino end groups.[36,37] Upon the addition of an excess of TCAI to the NMR solutions (DMSO-d_6) of these adamantane-modified PPGs, no such a downfield shift was observed, showing there was no free amino group in the modified PPG molecules, and the terminal amino groups of the starting PPGs were quantitatively derivatized with adamantyl groups. The selected characterization data including number-average molecular weight (M_n) and the polydispersity index (PDI: M_w/M_n) for the final adamantyl-containing PPGs as well as the corresponding starting PPGs are summarized in Table S1 (see Supporting Information).

2.2. Host−Guest Inclusion Complexation between β-CD-Core Star Polymer and Bis(adamantyl)-Terminated PPGs. *2.2.1. Thermoresponsive Behavior of the Host−Guest Self-Assembling System.* In this study, the interesting dual thermoresponsive behavior was investigated for the host−guest systems comprising of polymeric host β-CD-(PNIPAAm)$_4$ and polymeric guest PPG-(Ad)$_2$ in aqueous solution. Regarding the solubility in water at room temperature, the host polymer was very soluble, while the guest polymers used in this study were poorly soluble, except for PPG-400-(Ad)$_2$, which was moderately soluble. When the two components were mixed together, the LCST of guest polymer increased dramatically, while the LCST of host polymer decreased upon the host−guest inclusion complexation between adamantyl moiety and β-CD core. The detailed experimental results for the aqueous mixtures of β-CD-(PNIPAAm)$_4$ and PPG-2K-(Ad)$_2$ are given below as a typical example.

Figure 1 shows the information on the thermoresponsive behavior of a series of aqueous mixtures of β-CD-(PNIPAAm)$_4$ and PPG-2K-(Ad)$_2$ with varied host/guest ratio, which was investigated by the cloud point technique. It can be seen from this figure that individual aqueous guest

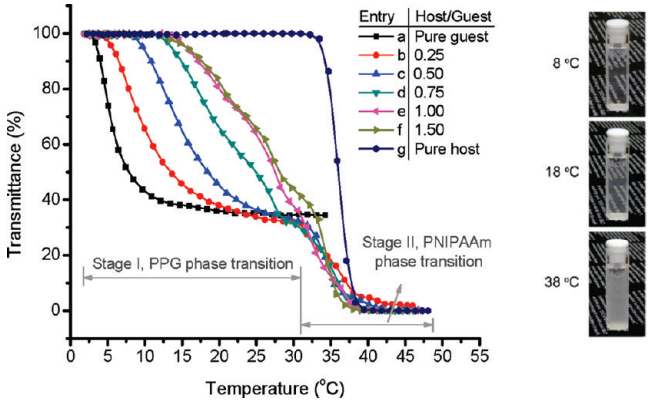

Figure 1. (left) Turbidity variations of aqueous solutions of PPG-2K-(Ad)$_2$ (guest polymer) as a function of temperature upon the addition of β-CD-(PNIPAAm)$_4$ (host polymer). $C_{guest\ polymer}$ = 0.26 mg/mL (for solutions a−f); $C_{host\ polymer}$ = 2.5 mg/mL (for solution g); host/guest represents the molar ratio of β-CD core/adamantyl moiety. (right) Representative photos of the 1:1 host−guest solution (e) at three typical temperatures (8, 18, and 38 °C).

(solution a) and host polymer (solution g) exhibited only single thermoresponsive profile, while host−guest systems (solutions b−f) exhibited interesting double thermoresponsive profiles, showing these systems underwent two stages of phase transition. This phenomenon is similar to those found in aqueous solutions of conventional copolymers containing two kinds of thermoresponsive blocks.[38−44] For these host−guest systems, stage I (below 31 °C) was closely related to the phase transition of PPG segment in the guest polymer, while stage II (above 31 °C) was due to the phase transition of PNIPAAm arms grafted onto the β-CD core of the host polymer. Representative photos of the 1:1 host−guest solution (e) at three typical temperatures (8, 18, and 38 °C) (Figure 1, right) clearly showed a turbidity change upon increasing the solution temperature.

Curve a in Figure 1 shows that the LCST of guest polymer PPG-2K-(Ad)$_2$ was ca. 5.6 °C. Herein, the LCST of the sample solution, which is equivalent to the cloud point of this solution, is defined as the temperature exhibiting a 34% decrease in optical transmittance of this solution at 500 nm in stage I due to PPG phase transition (i.e., half of the total decrease in stage I). The LCST of this guest polymer solution shifted to a higher temperature upon the addition of the macromolecular host, β-CD-(PNIPAAm)$_4$ (Figure 1, curves b−f). The LCST significantly changed with a LCST increase (ΔLCST, referenced to pure guest polymer) of 4.3 °C when the host/guest ratio, i.e., β-CD core/adamantyl moiety molar ratio, was 0.25. The ΔLCST further increased another 4.9 °C, resulting in an LCST of ca. 14.8 °C when the host/guest ratio reached 0.5. The LCST of this self-assembling system was ca. 20.0 and 24.2 °C when the host/guest ratio reached 0.75 and 1.0, respectively. However, the LCST became almost saturated upon further increase in the host/guest ratio beyond 1.0, indicating that the self-assembling system involved a 1:1 complexation between adamantyl moiety and β-CD core. The bis(adamantyl)-terminated PPG-2K could be incorporated to the β-CD core of the star polymer via inclusion complexation to form a supramolecular block copolymer (pseudo-block copolymer). Through forming the pseudo-block copolymer, the hydrophilic PNIPAAm arms on host polymer contributed to increase the water solubility of the guest polymer. In stage I, the LCST of the self-assembling system could be easily tuned through changing the host/guest ratio, i.e., the composition ratio of hydrophilic PNIPAAm/hydrophobic PPG like in conventional amphiphilic block copolymer systems. It

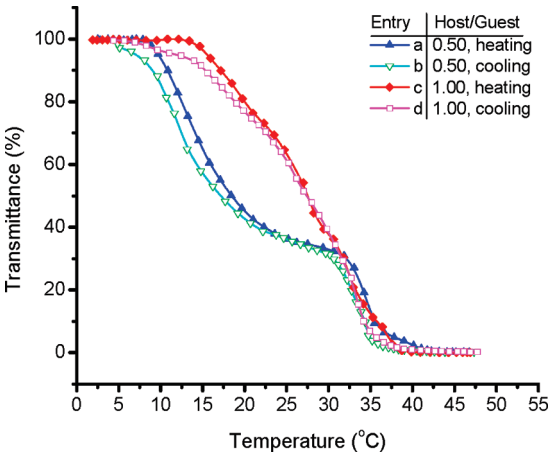

Figure 2. Turbidity variations of the host−guest system comprising PPG-2K-$(Ad)_2$ and β-CD-$(PNIPAAm)_4$ with the host/guest ratio of 0.5 and 1.0 during the temperature heating-up (solid symbol) and cooling-down (open symbol) processes. $C_{\text{guest polymer}}$ = 0.26 mg/mL.

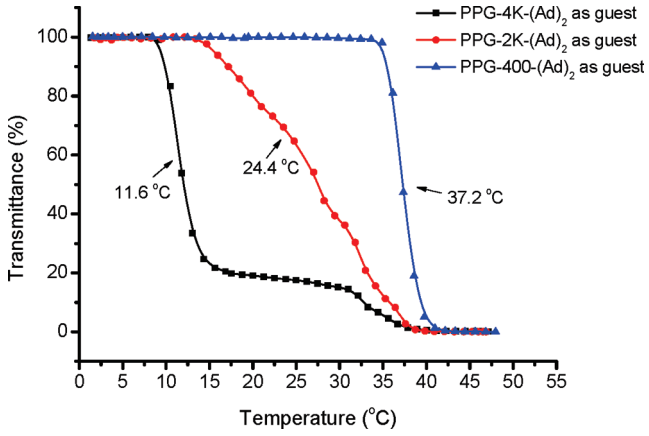

Figure 3. Turbidity variations of 1:1 host−guest systems comprising of β-CD-$(PNIPAAm)_4$ (host polymer) and different macromolecular guests as a function of temperature. Concentration of the mixtures, $C_{\text{host-guest}}$ = 2.0 mg/mL.

was also found that, by increasing the host/guest ratio, the transition range of PPG for the self-assembling systems (Figure 1, curves b−f) became less sharp than that for pure PPG guest solution (Figure 1, curve a), indicating that the aggregation process of PPG in these self-assembling systems was different than that in pure PPG guest solution. This was related to the formation of noncovalently connected micelles described in section 2.3. A similar phenomenon was also observed in conventional thermosensitive copolymer systems. For example, for narrow-dispersed PNIPAAm-based (co)polymers, incorporation of a hydrophobic moiety or block usually resulted in a lower LCST and a broader transition range of PNIPAAm.[45−47] By contrast, incorporation of a hydrophilic moiety or block usually resulted in a higher LCST and a broader transition range of PNIPAAm.[48,49]

In stage II, all host−guest solutions (b−f) exhibited a similar LCST around 34.7 °C due to the phase transition of PNIPAAm arm on host polymer. This value was a little lower than that of pure aqueous host polymer (35.9 °C, g) with the concentration of 2.5 mg/mL because of the decrease in water solubility of the host polymer upon inclusion complexation with PPG-2K-$(Ad)_2$. The two-stage transition was complete thermo-reversible for the host−guest systems. Two representative examples are shown in Figure 2 when the host/guest molar ratio was 0.5 and 1.0. It can be seen that the heating-up curves matched well with cooling-down curves in the turbidity test.

Subsequently, we investigated the effect of the PPG chain length of the adamantyl-containing PPGs on the LCST behaviors of the host−guest systems. In the case of PPG-4K-$(Ad)_2$, the trend of change in LCST of the systems with varying the host/guest ratio was quite similar to the case when PPG-2K-$(Ad)_2$ was used as guest polymer. A more clearly dual thermoresponsive behavior of these systems could be observed (see Supporting Information, Figure S1). By contrast, when PPG-400-$(Ad)_2$ was used as macromolecular guest, the systems did not show any dual thermoresponsive behavior (see Supporting Information, Figure S2), indicating that the effect of PPG chain length is significant.

As seen in Figure 3, for the 1:1 host−guest systems with same β-CD-$(PNIPAAm)_4$ host but different guest polymers, the LCST values were 11.6, 24.4, and 37.2 °C when PPG-4K-$(Ad)_2$, PPG-2K-$(Ad)_2$, and PPG-400-$(Ad)_2$ were used as macromolecular guest, respectively (in all cases, the total concentration was fixed to be 2.0 mg/mL). It can be concluded that the longer the PPG chain was, the lower the LCST was, as well as the more obvious the dual thermoresponsive behavior of the host−guest system was.

2.2.2. Two-Dimensional NOESY NMR Measurement. To further confirm the host−guest complexation of the β-CD-core-containing star-shaped PNIPAAm with the adamantyl-containing PPGs, 2D-NOESY NMR measurements were carried out. Herein, the 1:1 mixture of β-CD-$(PNIPAAm)_4$ and PPG-2K-$(Ad)_2$ in deuterated water was used as a representative sample (Figure 4). It was clearly found that the methine protons (*H*b) and the methylene protons (*H*c) of adamantyl moiety correlated well with both of the inner protons C(3)*H* and C(5)*H* of β-CD core, which were located on the wider and narrower side of β-CD core, respectively. However, the correlation peaks between methylene protons of adamantyl moiety, *H*a, and the inner protons C(3)*H* and C(5)*H* of β-CD core were not clear. All these results indicated that in this case, where the guest molecule possessed two adamantyl end groups, the adamantyl end formed complex from the wider side of the β-CD core.[20]

2.3. Formation of Noncovalently Connected Micelles. *2.3.1. NMR Spectroscopy Investigation.* In this study, the special micelles formed in host−guest self-assembling systems were investigated by using the NMR technique, which is a very popular method to study the effect of solvent on the structure of micelle formed from conventional amphiphilic diblock/triblock copolymers.[50−53] It was found that $CDCl_3$ was a good nonselective solvent for both the macromolecular host (star-shaped PNIPAAm with a β-CD core) and macromolecular guests (bis(adamantyl)-terminated PPGs), while D_2O was a good selective solvent for hydrophilic host polymer but poor solvent for hydrophobic guest polymers.

Herein, the 1:1 mixture of β-CD-$(PNIPAAm)_4$ and PPG-2K-$(Ad)_2$ was used as a representative sample. In $CDCl_3$, the peaks due to the PPG segment (δ 3.30−3.70 ppm), PNIPAAm segment (δ 1.13, 3.99 ppm), and adamantyl moiety (δ 1.60−2.00 ppm) were well-resolved at room temperature, and the resonance pattern did not change with temperature ranging from 8 to 38 °C (Figure 5, upper left). By contrast, in D_2O at room temperature, PNIPAAm signals at δ 1.09 and 3.84 ppm were still sharp and well-resolved; however, the signals due to the PPG segment at δ 3.20−3.60 ppm turned into broad and poorly resolved peaks. The signals due to

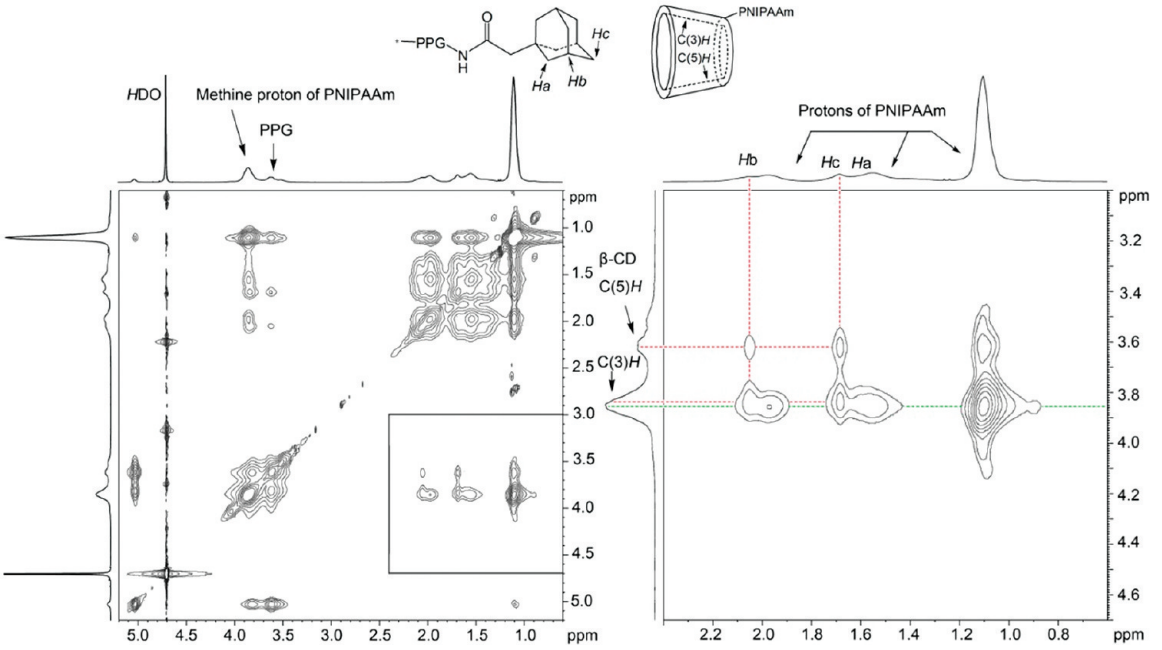

Figure 4. The full-scale (left) and selected-scale (right) 2D-NOESY NMR spectra of a 1:1 host−guest mixture of β-CD-(PNIPAAm)$_4$ and PPG-2K-(Ad)$_2$ in D_2O at 18 °C (300 MHz).

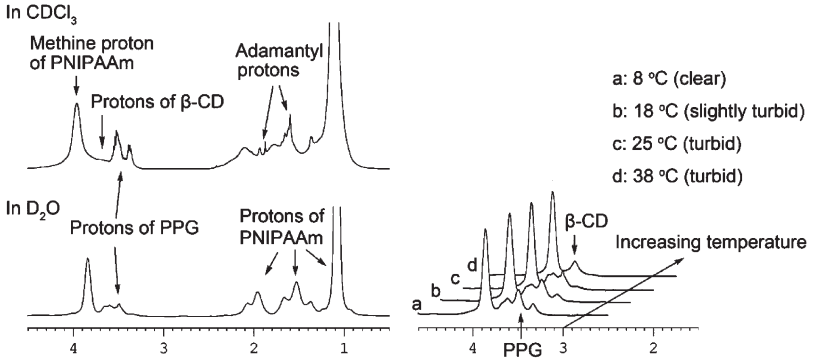

Figure 5. (left) ^{1}H NMR spectra of 1:1 mixture of β-CD-(PNIPAAm)$_4$ and PPG-2K-(Ad)$_2$ in $CDCl_3$ (upper) and D_2O (lower) at 25 °C, respectively. (right) Temperature-variable ^{1}H NMR spectra of 1:1 mixture of β-CD-(PNIPAAm)$_4$ and PPG-2K-(Ad)$_2$ in D_2O at (a) 8, (b) 18, (c) 25, and (d) 38 °C. Concentration of the mixtures, $C_{\text{host-guest}} = 2.0$ mg/mL.

adamantyl moiety were invisible under this condition, which may be hidden by the relatively strong signals of the main-chain methylene and methine protons of PNIPAAm at δ 1.30−2.40 ppm (Figure 5, lower left). Interestingly, a temperature-dependent resonance pattern was observed for the 1:1 host−guest mixture in D_2O, which was corresponding to the formation of noncovalently connected micelles (Figure 5, right).

According to the LCST behavior of the 1:1 host−guest mixture described in Figure 1, the mixture was clear at 8 °C. From the ^{1}H NMR spectrum (Figure 5, right, a), it was found that the peaks ascribed to both the PNIPAAm and PPG were sharp because the two segments could interact freely with surrounding deuterated water molecules under this condition. When the temperature was increased, the mixture turned from clear to slightly turbid (18 °C) and then turbid (25 and 38 °C) (Figure 1). During this process, PNIPAAm was still shown as sharp peaks. However, the peak intensity due to PPG segment decreased gradually with increasing temperature (Figure 5, right, b−d). This observation result was attributed to the restriction of the molecular motion of PPG segment in guest polymer, resulting from the reason that PPG segment became more and more hydrophobic in water at higher temperatures. This result also indicated the formation of core−corona micelle with a relatively hydrophobic core made up of guest polymer PPG-2K-(Ad)$_2$ and a hydrophilic outer corona made up of star-shaped PNIPAAm in water under higher temperature (>8 °C).[50,51,53]

2.3.2. Fluorescence Probe Investigation. The fluorescence probe technique has been widely used as a powerful tool to study micellar properties of conventional amphiphilic block copolymers.[54,55] It was known that both emission and excitation spectra of pyrene undergo significant changes upon micellization of block copolymers in an aqueous solution of pyrene (usually, 6×10^{-7} M). These changes are caused by the transfer of pyrene molecules from the polar aqueous environment to the hydrophobic micellar cores and are related to the location of the pyrene molecules in the solution. One important change should be noted is that the fluorescence excitation spectrum of pyrene shows a shift of the low-energy band of the La ($S_2 \leftarrow S_0$) from ca. 333 to 338 nm. It has been reported that this (0,0) absorption band change of pyrene is more sensitive to the true onset of

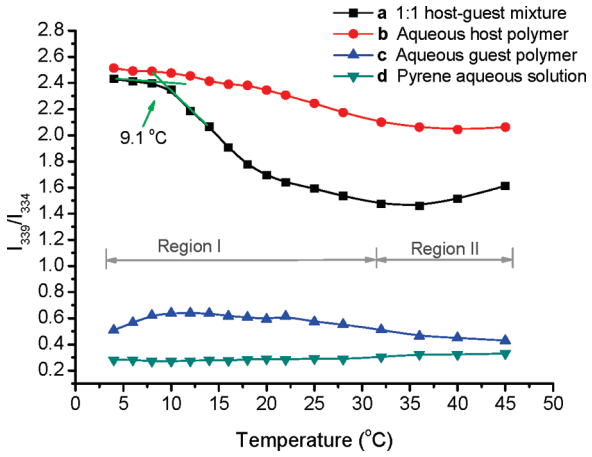

Figure 6. Plots of the I_{339}/I_{334} ratio of pyrene excitation spectra as a function of temperature in (a) 1:1 host−guest mixture of β-CD-(PNIPAAm)$_4$ and PPG-2K-(Ad)$_2$ ($C_{host-guest}$ = 2.0 mg/mL), (b) aqueous solution of β-CD-core star-shaped PNIPAAm (control 1, C_{host} = 1.74 mg/mL), (c) aqueous suspension of PPG-2K-(Ad)$_2$ (control 2, C_{guest} = 0.26 mg/mL), and (d) pyrene aqueous solution (control 3). The steady-state fluorescence excitation spectra were monitored at 373 nm. The concentration of pyrene is 6.0×10^{-7} M.

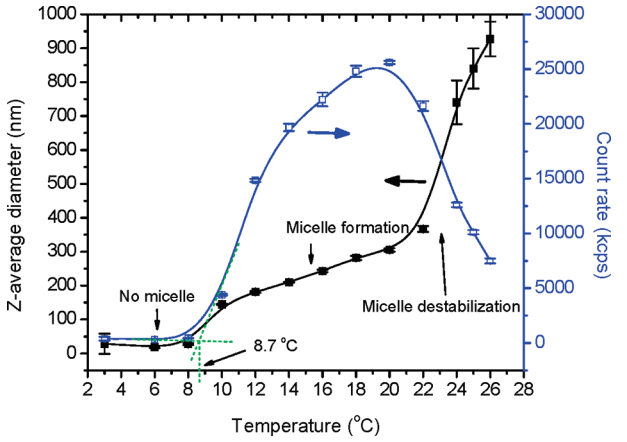

Figure 7. Micelle size and scattered light intensity of the 1:1 host−guest system of β-CD-(PNIPAAm)$_4$ and PPG-2K-(Ad)$_2$ as a function of temperature in water. Total concentration of the system: $C_{host-guest}$ = 2.0 mg/mL.

aggregation than either lifetime measurements or fluorescence emission changes.[56,57] This change is described in terms of the ratio of the intensities of the two bands at ca. 338 and 333 nm in the pyrene fluorescence excitation spectrum.

In this study, the thermosensitive micellization behavior of the 1:1 host−guest system of β-CD-(PNIPAAm)$_4$ and PPG-2K-(Ad)$_2$ was determined as a representative example by using the fluorescence excitation spectra of the pyrene probe. The two excitation bands of pyrene were centered at 334 and 339 nm in our system. Figure 6a shows the intensity ratio of I_{339}/I_{334} of pyrene excitation spectra as a function of temperature for this 1:1 host−guest system. Aqueous solution of host polymer (Figure 6b), aqueous suspension of guest polymer (Figure 6c), and pyrene aqueous solution (Figure 6d) were used as controls. The intensity ratio of I_{339}/I_{334} versus temperature for the 1:1 host−guest system showed a clear reverse sigmoid curve. By comparison, only a little change in the ratio of I_{339}/I_{334} was observed for the three control systems.

According to the results of turbidity experiments described in Figure 1, the curve for the 1:1 host−guest mixture in Figure 6 would be divided into two distinctive regions. Region I (4−32 °C) was relevant to the phase transition of PPG block in the guest polymer. At the beginning of this region (below 8 °C), the host−guest solution was clear and the ratio of I_{339}/I_{334} was stable at ca. 2.4. This value of I_{339}/I_{334} ratio was slightly lower than that in pure host polymer solution (ca. 2.5, Figure 6b) but much higher than those in pure guest polymer suspension (ca. 0.5−0.65, Figure 6c) and pure pyrene aqueous solution (ca. 0.28, Figure 6d). In the case of pure host polymer solution, pyrene molecules were mainly encapsulated into the hydrophobic β-CD cavity of the host polymer, which resulted in the highest ratio of I_{339}/I_{334} among the four systems under study. In the case of 1:1 host−guest mixture, the partition of pyrene inside the hydrophobic β-CD cavity was lower than that in pure host polymer solution because of the presence of adamantane-containing guest polymer. Adamantyl moiety was known to fit better into the β-CD cavity than pyrene. While in the case of pure guest polymer suspension, the ratio of I_{339}/I_{334} was very low (near the corresponding value in pure pyrene aqueous solution) because pyrene molecules stayed in a polar microenvironment. The ratio of I_{339}/I_{334} in this case was similar to the reported results for pyrene in some triblock copolymers solutions at low concentration range (i.e., before the micelles were formed).[45,56,58] However, a dramatic fall of I_{339}/I_{334} occurred in the 1:1 host−guest solution when the temperature was further increased, and this ratio dropped to the lowest value when temperature reached ca. 32 °C. The decrease in I_{339}/I_{334} ($\Delta(I_{339}/I_{334})$, referenced to the initial value, 2.4, at 4 °C) was ca. 1. The abrupt change of I_{339}/I_{334} was indicative for the formation of noncovalently connected micelle. The increased temperature of the system resulted in the formation of hydrophobic micellar core composed of aggregated PPG chains. During the micellization, pyrene molecules transferred from the hydrophobic β-CD cavity of the host polymer to the relatively less hydrophobic core of the noncovalently connected micelle, which caused abrupt decrease in the intensity ratio of I_{339}/I_{334}. By comparison, no such an abrupt $\Delta(I_{339}/I_{334})$ was observed with increasing temperature for pure host polymer solution as well as pure guest polymer suspension. According to curve a in Figure 6, the critical micelle temperature (CMT) for this thermoresponsive 1:1 host−guest mixture was calculated to be 9.1 °C, which was defined as the temperature point with an abrupt decrease in the ratio of I_{339}/I_{334}. A slowdown of the decrease in I_{339}/I_{334} was observed when the temperature was raised to around 32 °C. The value of I_{339}/I_{334} around this temperature was ca. 1.5, which was similar to some reported results for pyrene in conventional triblock copolymers solutions at high concentration range (i.e., after the micelles were formed).[45,56,58]

Region II (32−45 °C) was relevant to the phase transition of PNIPAAm block in the host polymer. The PNIPAAm chains began to collapse and aggregate, and the micellar system lacked the protection of hydrophilic shell was gradually destroyed. In this region, a little increase in I_{339}/I_{334} was found for both the 1:1 host−guest system and pure host polymer solution, while a little decrease in I_{339}/I_{334} was found for pure guest polymer suspension. For the pyrene aqueous solution, the ratio of I_{339}/I_{334} was almost constant over the temperature range of 4−45 °C.

2.4. Size and Morphology of Noncovalently Connected Core−Shell Micelles. The size of micelles is an important factor to determine the applications. The uptake characteristics of any drug encapsulated in micelle will be affected by the micellar size and morphology.[3] In this study, the size distribution and morphology of the noncovalently connected core−shell micelles were investigated by DLS, TEM, and

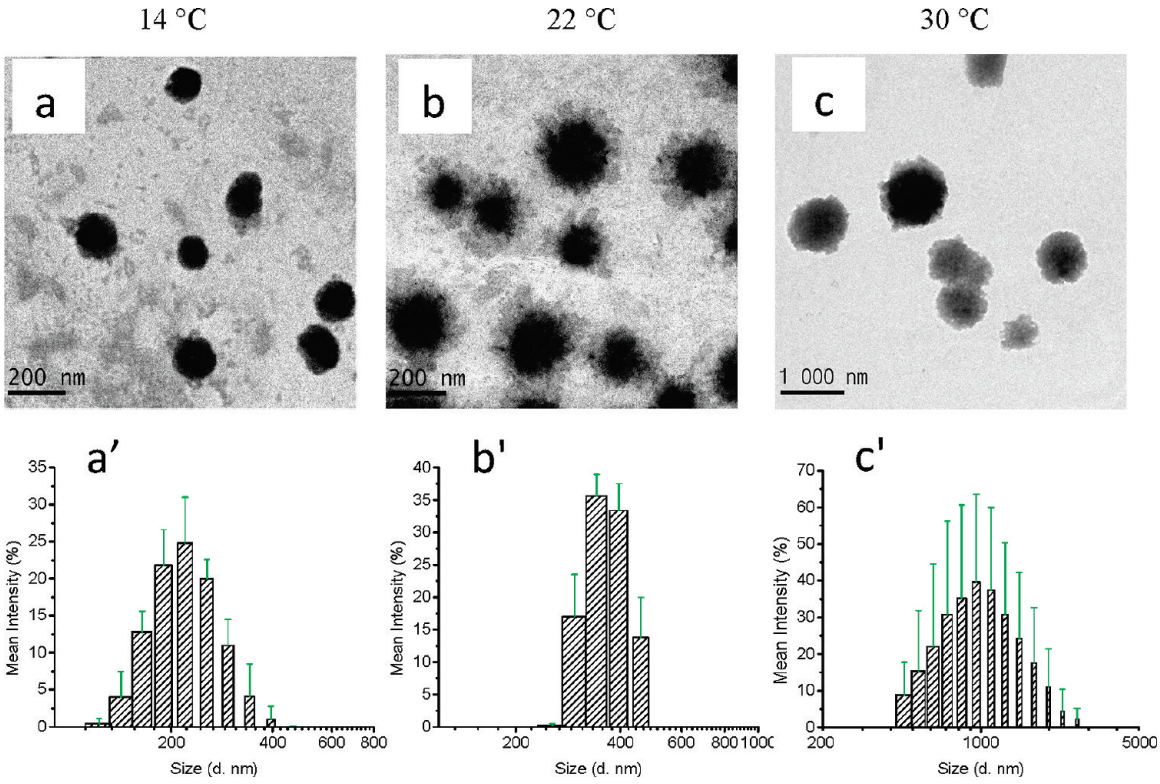

Figure 8. (top) Representative TEM micrographs of the noncovalently connected micelles formed from 1:1 host−guest mixture of β-CD-core star-shaped PNIPAAm and PPG-2K-$(Ad)_2$ at 14, 22, and 30 °C (a−c). (bottom) Histogram showing the size distribution of the noncovalently connected micelles by DLS at 14, 22, and 30 °C from three individual measurements (a′−c′). Concentration of the 1:1 host−guest mixture: $C_{host-guest}$ = 2.0 mg/mL.

AFM observation, respectively. Meanwhile, DLS was proved to be a sensitive method to trace the formation of noncovalently connected core−shell micelle according to the change in particle size and scattered light intensity in the 1:1 host−guest system. The result from DLS study was consistent with that from fluorescence probe investigation.

The changes of micelle size and count rate with temperature (3−26 °C) for the 1:1 host−guest system of β-CD-$(PNIPAAm)_4$ and PPG-2K-$(Ad)_2$ are shown in Figure 7. The scattered light intensity was given here in kilocounts per second (kcps). It can be seen that the values of both micelle size and count rate were very small and kept unchanged under lower temperature (< 8 °C). However, the two values increased dramatically when the temperature was increased above 8 °C. The increase in count rate could be attributed to a change in the refractive index of the guest molecule as its PPG block underwent a phase transition from random coil to condensed globule. The latter structure of PPG possessed higher refractive index than that of the former one. This change indicated clearly that the micelles began to form at around 8 °C. According to the curve of count rate versus temperature, the critical micelle temperature (CMT) was calculated to be 8.7 °C, which was very close to that obtained from fluorescence probe investigation earlier (9.1 °C).

In the temperature range from 10 to 20 °C, the count rate increased rapidly from 4.4×10^3 to 2.6×10^4 kcps, while the average micelle diameter increase slowly from 150 to 300 nm, showing that the noncovalently connected micelles were relatively stable in this temperature range. In this stage, the host−guest solution was observed to be slightly turbid and was very faint blue according to the turbidity experiments described earlier. At each temperature, the size of the resultant micelle with very narrow polydispersities (ca. 0.1−0.2) could remain constant, and the system did not form aggregates for at least 1 day. When temperature reached to above 22 °C, a rapid increase in particle size and a corresponding rapid decrease in count rate were observed. Meanwhile, the mixture became very turbid, showing clearly the destabilization of the noncovalently connected micelles. In this temperature range, micelles aggregation and precipitation occurred.

Figure 8 shows the representative TEM micrographs of noncovalently connected micelles formed from 1:1 host−guest mixture of β-CD-core star-shaped PNIPAAm and PPG-2K-$(Ad)_2$ at 14, 22, and 30 °C, respectively. From TEM micrographs, smaller spherical particles (ca. 110−160 nm in diameter) were observed for sample solution prepared and dried at 14 °C (Figure 8a), whereas bigger spherical particles (ca. 200−300 nm in diameter) were observed for sample solution prepared and dried at 22 °C (Figure 8b), showing that the noncovalently connected micelles formed at higher temperature had bigger size. These micelles were well-dispersed as individual nanoparticles. In comparison, very big particles with diameter of ca. 1 μm were observed in the case of 30 °C (Figure 8c). These results supported the observations made with DLS mentioned above (as seen in Figure 7). From the TEM images, a dense dark core and a less dense corona could be observed, which was especially clear for the sample prepared and dried at 22 °C. This was due to the action of the staining agent, phosphotungstic acid, which stains the hydrophobic core (PPG) to a greater extent. The TEM micrographs also showed a narrow size distribution of the noncovalently connected micelles formed at 14 and 22 °C. This was consistent with the observation from DLS, which gave very narrow polydispersity of the micelle size of ca. 0.1 for the two samples (Figure 8, a′ and b′). However, for the micelles formed at 30 °C, the particle size distribution was very broad due to the micelle aggregation at this temperature (Figure 8, c and c′). It was found that the diameters of the micelles from the TEM micrographs were clearly smaller than those from DLS measurements. This could be related to

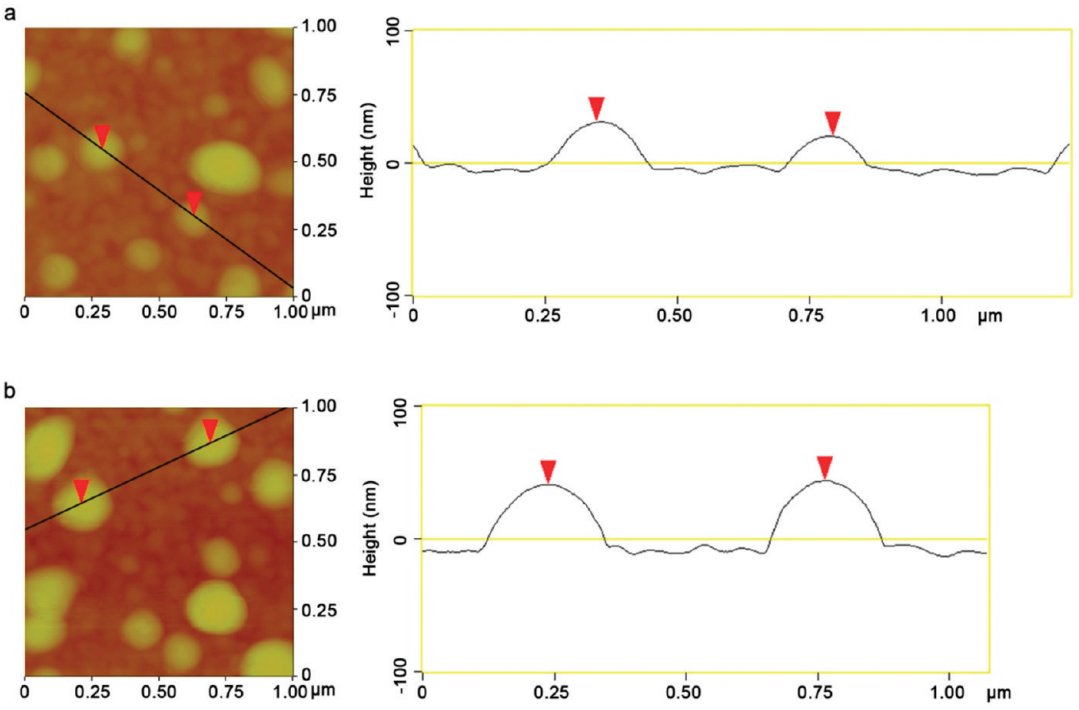

Figure 9. Representative AFM images and corresponding line profiles of the noncovalently connected micelles formed from 1:1 host−guest solution of β-CD-core star-shaped PNIPAAm and PPG-2K-$(Ad)_2$ at 14 °C (a) and 22 °C (b). Concentration of the 1:1 host−guest solution: $C_{host-guest}$ = 2.0 mg/mL.

Scheme 2. Schematic Drawing Showing the Formation of Pseudo-Block Copolymer and Noncovalently Connected Micelles as Well as Micelle Destabilization in a 1:1 Host−Guest Mixture with Increasing Temperature

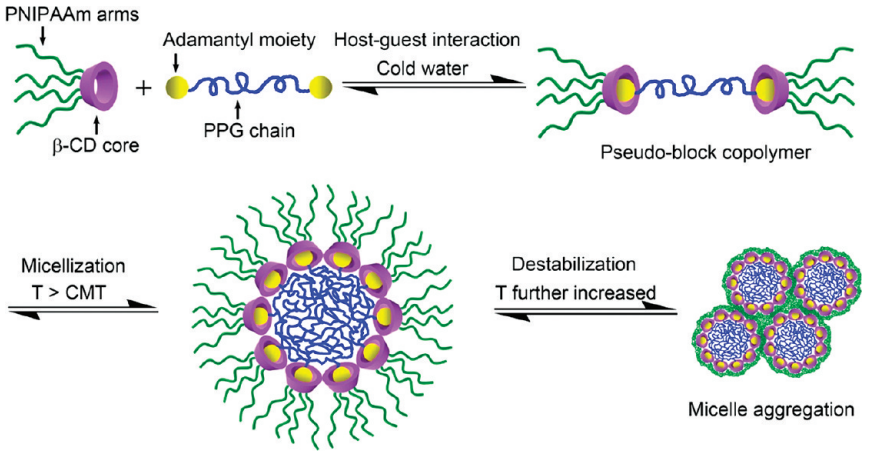

the fact that DLS measures the hydrodynamics diameter of the micelles in an aqueous environment whereas the TEM micrographs show the dehydrated solid state of the micelles.

The size and shape of the noncovalently connected micelles formed from the 1:1 host−guest solution of β-CD-core star-shaped PNIPAAm and PPG-2K-$(Ad)_2$ were further measured in the solid state by AFM (Figure 9). The AFM observation gave the mean micelles diameter around 180 and 220 nm for the samples prepared and dried at 14 and 22 °C, respectively. These results were in accordance with those found in TEM images.

On the basis of our extensive study on the 1:1 host−guest mixture of β-CD-core star-shaped PNIPAAm and PPG-2K-$(Ad)_2$ by a combination of ^{1}H NMR, 2D-NOESY NMR, fluorescence probe technique, DLS, TEM, and AFM, a mechanism for the self-assembly and thermosensitive micellization of the pseudo-block copolymer under study was proposed (Scheme 2). It can be seen from Scheme 2 that the 1:1 host−guest mixture containing two kinds of thermoresponsive blocks underwent a thermoreversible transition from free pseudo-block copolymer to stable noncovalently connected micelles and then to unstable aggregates by changing the temperature in the range of 2−45 °C. Considering potential applications, the thermo-induced micellization step (related to the phase transition of PPG) has more interest than the micelle aggregation step (related to the phase transition of PNIPAAm) in this study.

We further studied the thermosensitive micellization behaviors of other host−guest systems with different host/guest ratio and PPG chain length. Some selected characterization data for these host−guest systems are summarized in Table 1. It was found from this table that LCST, CMT, mean diameters of resultant micelles, and the size polydispersity were greatly dependent on the PPG chain length of guest

Table 1. Solution Properties of Polymeric Host−Guest Systems Comprising of β-CD-Core Star-Shaped PNIPAAm and Bis(adamantyl)-Terminated PPGs

guest polymer	host/guest	$C_{host-guest}$ (mg/mL)	LCST (°C)[a]	CMT (°C)[b]	*d*, 14 °C (nm)[c]	*d*, 22 °C (nm)[c]
PPG-400-$(Ad)_2$	1.0	2.0	37.2	31.0	solution	solution
PPG-2K-$(Ad)_2$	1.0	2.0	24.4	8.7	210 ± 1 (0.10)	367 ± 9 (0.10)
PPG-2K-$(Ad)_2$	1.0	0.6	33.0	18.0	71 ± 4 (0.42)	148 ± 1 (0.22)
PPG-2K-$(Ad)_2$	0.5	1.1	15.6		790 ± 33 (0.64)	1458 ± 90 (1.00)
PPG-2K-$(Ad)_2$	1.5	2.9	24.9	11.0	345 ± 17 (0.38)	1149 ± 33 (0.94)
PPG-4K-$(Ad)_2$	1.0	2.0	11.6	4.0	1190 ± 55 (0.99)	aggregation

[a] Determined by means of the cloudy point technique. [b] Critical micelle temperature is experimentally described in the present study by an abrupt increase in the mean count rate. [c] Mean *Z*-average diameters by dynamic light scattering from three individual measurements. Numbers in parentheses represent the average polydispersity of the particle size.

polymer, host/guest ratio, and system concentration and were tunable by easily changing the composition of the self-assembling systems.

3. Conclusions

A polymeric host−guest system was designed using star-shaped PNIPAAm with a β-CD core and bis(adamantyl)-terminated PPGs, which was able to form ABA-type dual thermo-responsive supramolecular pseudo-block copolymers in aqueous solution via host−guest complexation between the β-CD core of the host polymer and the adamantyl moieties of the guest polymers. The pseudo-block copolymers showed tunable LCST behavior in aqueous solution by varying the host/guest ratio up to 1.0. The pseudo-block copolymers could self-assemble into non-covalently connected micelles with the PPG segment as the core and hydrophilic PNIPAAm-grafted β-CD as the corona. Typically, a 1:1 host−guest mixture of β-CD-core star PNIPAAm and PPG-2K-$(Ad)_2$ reversibly experienced the change from clear solution (below 8 °C, no micelle) to slightly turbid solution (10−20 °C, micelle formation) and then to turbid mixture (above 22 °C, micelle destabilization).

The critical micelle temperature (CMT) of the host−guest system was dependent on the composition and concentration of the components. The size of the resultant noncovalently connected micelle could be easily tuned not only by changing the temperature, the concentration of the system, but also through changing the ratio of host/guest and the length of the PPG chain, which provided more rooms to manipulate and control the micelle formation as compared to that in conventional amphiphilic copolymer.

This kind of supramolecular pseudoblock copolymers formed from host−guest complexation has great potential for drug delivery applications owing to their tunability of thermoresponsive behavior, noncovalent connected micelle-forming ability, and their potential biocompatibility.

4. Experimental Section

4.1. Materials. β-Cyclodextrin (98%) was purchased from Sigma and used after recrystallization from water and drying at 100 °C under vacuum. *N*-Isopropylacrylamide (Aldrich, 99%) was recrystallized twice from hexane before use. Copper(I) bromide (Fluka, 98%) was washed with glacial acetic acid in order to remove any soluble oxidized species, filtered, washed with ethanol, and dried. 2-Bromoisobutyric bromide (99%), anhydrous *N*,*N*-dimethylacetamide (99%), adamantaneacetic acid (98%), *N*,*N*′-dicyclohexylcarbodiimide (DCC, 1.0 M in methylene chloride), and trichloroacetyl isocyanate (TCAI) (96%) were all purchased from Aldrich. 4-(Dimethylamino)-pyridine (DMAP, >99%) was purchased from Fluka. Poly(propylene glycol) bis(2-aminopropyl ether)s with average molecular weight of 400 Da (NH_2-PPG-400-NH_2), 2000 Da (NH_2-PPG-2K-NH_2), and 4000 Da (NH_2-PPG-4K-NH_2) were obtained from Aldrich. Methylene chloride was distilled over CaH_2 before use. Tris[2-(dimethylamino)ethyl]amine (Me_6-TREN) was prepared according to the literature.[59] All other reagents were used as received without further purification.

4.2. Synthesis of Star-Shaped PNIPAAm with a β-CD Core via Atom Transfer Radical Polymerization (ATRP). *a. Synthesis of β-CD-Based Macroinitiator (4Br-β-CD).* β-CD (5.11 g, 4.5 mmol) was dissolved in 30 mL of anhydrous *N*,*N*-dimethylacetamide with stirring and then was cooled to 0 °C. Subsequently, a solution of 2-bromoisobutyric bromide (4.14 g, 18.0 mmol) in anhydrous *N*,*N*-dimethylacetamide (10 mL) was added dropwise to the β-CD solution for a period of 1 h at 0 °C under a N_2 atmosphere with rapid stirring. After the addition, the reaction temperature was maintained at 0 °C for another 2 h and then allowed to rise slowly to room temperature, after which the reaction was allowed to continue for 24 h. The final reaction mixture was precipitated with 900 mL of diethyl ether. The resulting white powder was collected by centrifugation and washed with acetone (2 × 30 mL). In the purification process, the crude product was suspended in 100 mL of deionized water, and the mixture was stirred at rt overnight. After that, the solid was collected by centrifugation, washed well with deionized water (2 × 30 mL) and acetone (2 × 30 mL), and then dried under vacuum at 40 °C. Yield 4.25 g (54.6%, based on a substitution degree of 4). FTIR (KBr): ν = 3383 (br, ν(O−H)), 2928 (m, ν(C−H)), 1736 (s, ν(C═O)), 1636 (m), 1286 (m), 1157 (s), 1104 (s), 1079 (s), 1030 (s, ν(C−O−C)), 947 (w), 759 (w), 704 (w), 649 (w, ν(C−Br)), 581 cm^{-1} (m). ^{1}H NMR (400 MHz, DMSO-d_6, δ): 1.88 (m, 24H, −OCO−C(CH_3)$_2$Br), 3.00−6.00 (m, 66H, −O*H* and −C*H*− of β-CD). ^{13}C NMR (100 MHz, DMSO-d_6, δ): 170.7, 170.5 (*C*═O), 102.5−101.3 (*C*(1) of β-CD), 81.9−80.5 (*C*(4) of β-CD), 73.1, 72.8 (*C*(3) of β-CD), 72.1 (*C*(2) of β-CD), 72.0 (*C*(5) of β-CD), 69.1, 69.0 (*C*(5′) of β-CD), 65.0, 64.4 (*C*(6′) of β-CD), 59.4 (*C*(6) of β-CD), 57.1 (*C*-Br), 30.4, 30.3 (*C*H_3). Anal. Calcd for $C_{58}H_{90}Br_4O_{39}\cdot 2H_2O$: C 39.42, H 5.36, Br 18.09. Found: C 37.96, H 5.46, Br 22.39.

b. ATRP of NIPAAm Using 4Br-β-CD as Macroinitiator. 4Br-β-CD (176.8 mg, 0.103 mmol) and NIPAAm (1.358 g, 12.0 mmol) were added into a dry flask. The flask was sealed with a septum and subsequently purged with dry nitrogen for several minutes. Then, Me_6-TREN (111.0 mg, 0.48 mmol) in 3.5 mL of thoroughly degassed methanol was added with a degassed syringe. The mixture was stirred at rt and purged with dry nitrogen for 10 min. Last, CuBr (57.4 mg, 0.4 mmol) was added, and the mixture was purged with dry nitrogen for another 10 min at rt. The mixture was then heated at 70 °C in an oil bath. After 4 h, the experiment was stopped by opening the flask and exposing the catalyst to air. The final green mixture was diluted with THF and passed through a short Al_2O_3 column to remove copper catalyst. The resulting eluate solution was concentrated to ca. 10 mL and precipitated with 500 mL of diethyl ether. The white product was collected by centrifugation, washed with diethyl ether, and dried under vacuum at 40 °C. Yield 672.8 mg (43.8%). FTIR (KBr): ν = 3394 (br, ν(O−H)), 3300 (br, ν(N−H)), 2975, 2936, 2878 (m, ν_s(C−H) and ν_{as}(C−H)), 1647 (s, ν(C═O), amide I), 1550 (s, ν(C−N) and δ(N−H), amide II), 1459 (m), 1388, 1369 (m, ν(C−N)), 1155 (m), 1081 (m), 1036 cm^{-1} (m, ν(C−O−C)). ^{1}H NMR (400 MHz, DMSO-d_6, δ): 1.04 (b, −CH(CH_3)$_2$), 1.44 (b, −CH_2−CH(CONH−)−), 1.96

(b, $-CH_2-CH(CONH-)-$), 3.50−4.00 (m, C(2)*H*−C(6)*H* of β-CD, overlapped with methine proton of isopropyl group), 3.84 (b, $-CH(CH_3)_2$), 4.30−4.90 (m, −O(6)*H* and C(1)*H* of β-CD), 5.60−5.90 (b, −O(2)*H* and −O(3)*H* of β-CD), 6.90−7.60 (b, −CON*H*−). ^{13}C NMR (100 MHz, D_2O, δ): 177.9 (*C*=O of NIPAAm unit), 105.0 (*C*(1) of β-CD), 83.6 (*C*(4) of β-CD), 71.1−75.9 (*C*(2), *C*(3) and *C*(5) of β-CD), 62.6 (*C*(6) of β-CD), 44.4−45.8 (*C*H of NIPAAm unit), 34.1−39.6 (CH_2 of NIPAAm unit), 24.3 (CH_3 of NIPAAm unit). Anal. Calcd for $C_{394}H_{706}Br_4N_{56}O_{95}$ (based on the number of arm n = 4 and number of repeating unit per arm m = 14): C 58.66, H 8.82, N 9.72. Found: C 58.33, H 9.52, N 10.10.

4.3. Synthesis of Adamantyl-Containing Poly(propylene glycol)s. These polymers were synthesized by coupling adamantaneacetic acid with corresponding PPGs. The procedure for the preparation of PPG-2K-$(Ad)_2$ from commercial (NH_2-PPG-2K-NH_2) and adamantaneacetic acid is given below as a typical example.

A mixture of NH_2-PPG-2K-NH_2 (2.0 g, 1.0 mmol) and DMAP (488.7 mg, 4.0 mmol) was dried under vacuum at 50 °C overnight. After being cooled to room temperature, a solution of adamantaneacetic acid (582.7 mg, 3.0 mmol) in 60 mL of anhydrous dichloromethane (DCM) was added with stirring. The reaction mixture was then heated to reflux, and the trace amount of water in the reaction mixture was removed by azeotropic distillation under a nitrogen atmosphere. When the residual solution in the reaction flask was about 8 mL, it was cooled to room temperature. Subsequently, a solution of DCC (5 mL, 1 mol/L) in DCM was added to the reaction mixture dropwise under stirring over a period of 5 min. Several minutes later, the byproduct dicyclohexylurea (DCU) precipitated as a white powder. After being stirred for another 48 h at room temperature, the final reaction mixture was filtered to remove insoluble DCU. The filtrate was concentrated to ca. 5 mL and then purified by passing through a Sephadex LH-20 column (2.5 × 40 cm) with methanol as eluent. Yield 1.5 g (75%). FTIR (film on NaCl plate): ν = 3319 (m, ν(N−H), amide), 2971, 2901 (s, ν_s(C−H) and ν_{as}(C−H)), 1650 (m, ν(C=O), amide I), 1536 (m, ν(C−N) and δ(N−H), amide II), 1109 cm^{-1} (s, ν(C−O−C)). ^{1}H NMR (400 MHz, $CDCl_3$, δ): 6.10−5.65 (br, 2H, −N*H*−CO−), 4.20−4.00 (br, 2H, −C*H*(CH_3)−NHCO−), 3.80−3.45 (m, 68H, −CH_2− in PPG chain), 3.45−3.30 (m, 32H, −C*H*(CH_3)− in PPG chain), 1.96 (br, 6H, methine protons of adamantyl group), 1.89 (s, 4H, −NHCO−CH_2−adamantyl), 1.75−1.60 (m, 24H, methylene protons of adamantyl group), 1.20−1.05 (102H, −CH_3− in PPG chain). ^{13}C NMR (100 MHz, $CDCl_3$, δ): 170.36 (−*C*O−NH−), 76.84−75.07 (−*C*H_2− in PPG chain), 73.59−72.18 (−*C*H(CH_3)− in PPG chain), 51.87 (−*C*H_2−adamantyl), 45.26 (−*C*H(CH_3)−NHCO−), 42.76, 36.96, 32.87, 28.81 (adamantyl group), 18.08−17.17 (−*C*H_3 in PPG chain).

PPG-400-$(Ad)_2$. Yield, 44.1%. FTIR (film on NaCl plate): ν = 3300 (m, ν(N−H), amide), 2970, 2902, 2849 (s, ν_s(C−H) and ν_{as}(C−H)), 1641 (s, ν(C=O), amide I), 1544 (m, ν(C−N) and δ(N−H), amide II), 1104 cm^{-1} (s, ν(C−O−C)). ^{1}H NMR (400 MHz, $CDCl_3$, δ): 6.10−5.65 (br, 2H, −N*H*−CO−), 4.20−4.00 (br, 2H, −C*H*(CH_3)−NHCO−), 3.80−3.25 (m, 17H, −CH_2−C*H*(CH_3)− in PPG chain), 1.96 (br, 6H, methine protons of adamantyl group), 1.90 (s, 4H, −NHCO−CH_2−adamantyl), 1.75−1.59 (m, 24H, methylene protons of adamantyl group), 1.20−1.05 (19H, −CH_3− in PPG chain). ^{13}C NMR (100 MHz, $CDCl_3$, δ): 170.37 (−*C*O−NH−), 76.84−75.30 (−*C*H_2− in PPG chain), 73.50−72.17 (−*C*H(CH_3)− in PPG chain), 52.06 (−*C*H_2−adamantyl), 45.26 (−*C*H(CH_3)−NHCO−), 42.79, 36.97, 32.87, 28.86 (adamantyl group), 18.08−17.19 (−*C*H_3 in PPG chain).

PPG-4K-$(Ad)_2$. Yield, 85.6%. FTIR (film on NaCl plate): ν = 2971, 2900 (s, ν_s(C−H) and ν_{as}(C−H)), 1651 (m, ν(C=O), amide I), 1528 (m, ν(C−N) and δ(N−H), amide II), 1108 cm^{-1} (s, ν(C−O−C)). ^{1}H NMR (400 MHz, $CDCl_3$, δ): 6.10−5.50 (br, 2H, −N*H*−CO−), 4.20−4.00 (br, 2H, −C*H*(CH_3)−NHCO−), 3.80−3.45 (m, 133H, −CH_2− in PPG chain), 3.45−3.30 (m, 65H, −C*H*(CH_3)− in PPG chain), 1.96 (br, 6H, methine protons of adamantyl group), 1.90 (s, 4H, −NHCO−CH_2−adamantyl), 1.75−1.58 (m, 24H, methylene protons of adamantyl group), 1.20−1.05 (200H, −CH_3− in PPG chain). ^{13}C NMR (100 MHz, $CDCl_3$, δ): 170.37 (−*C*O−NH−), 76.84−75.08 (−*C*H_2− in PPG chain), 73.52−72.18 (−*C*H(CH_3)− in PPG chain), 52.06 (−*C*H_2−adamantyl), 45.27 (−*C*H(CH_3)−NHCO−), 42.78, 36.96, 32.88, 28.85 (adamantyl group), 18.08−17.16 (−*C*H_3 in PPG chain).

4.4. Measurements and Characterization Methods. *General.* Gel permeation chromatography (GPC) analysis was carried out with a Shimadzu SCL-10A and LC-8A system equipped with two Phenogel 5 μ 50 and 1000 Å columns (size: 300 × 4.6 mm) in series and a Shimadzu RID-10A refractive index detector. Tetrahydrofuran (THF) was used as eluent at a flow rate of 0.20 mL/min at 45 °C. Monodispersed poly(ethylene glycol) (PEG) standards were used to obtain a calibration curve. Proton and carbon nuclear magnetic resonance (^{1}H and ^{13}C NMR) spectra were recorded at room temperature on a Bruker Avance DRX 400 MHz NMR spectrometer operating at 400.1 and 100.6 MHz, respectively. Chemical shifts were reported in parts per million (ppm) on the δ scale and were referenced to residual protonated solvent peaks: $CDCl_3$ spectra were referenced to C*H*Cl_3 at δ_H 7.26 and *C*DCl_3 at δ_C 77.36; D_2O spectra were referenced to *H*DO at δ_H 4.70; DMSO-d_6 spectra were referenced to (C*H*D_2) (CD_3)SO at δ_H 2.50. The 2D-NOESY (two-dimensional nuclear Overhauser effect spectroscopy) NMR experiments were performed at 300 MHz in D_2O on a Bruker Avance DRX 300 MHz NMR spectrometer with sodium 3--(trimethylsilyl)propane-1-sulfonate as reference. Fourier transform infrared (FTIR) spectra of samples in KBr pellet or deposited on surface of NaCl plate were recorded on a Perkin-Elmer FTIR 2000 spectrometer in the region of 4000−400 cm^{-1}; 64 scans were signal-averaged with a resolution of 2 cm^{-1} at room temperature. The X-ray photoelectron spectroscopy (XPS) measurements were performed on a Kratos AXIS HSi spectrometer equipped with a monochromatized Al Kα X-ray source (1486.6 eV photons). Elemental analyses were carried out using a Perkin-Elmer 2400 CHN/CHNS elemental analyzer.

Lower Critical Solution Temperature (LCST) of Host−Guest Self-Assembling Systems. A predetermined amount of bis(adamantyl)-terminated PPGs (guest polymers) and a corresponding amount of β-CD-core star-shaped PNIPAAm (host polymer) were dissolved in 1 mL of distilled water, and the transmission changes of the self-assembling system (in a 1 cm sample cell referenced against distilled water) at 500 nm were followed by using a UV−vis spectrophotometer (Shimadazu UV-2501PC) equipped with a Fisher Scientific Isotemp 1013P circulating water bath in the temperature range of 2−50 °C at various temperatures (heating rate: 1.2 °C/min; cooling rate: 0.5 °C/min; however, the heating and cooling rate was 0.12 °C/min at the temperature range between 3 °C below and above the LCST). The LCST of host−guest solution, which is equivalent to its cloud point, is defined as the temperature exhibiting half of the total decrease in optical transmittance of the solution at 500 nm in stage I due to PPG phase transition.

Critical Micelle Temperature Determination of Host−Guest Self-Assembling Systems by Fluorescence Spectroscopy. Steady-state fluorescence spectra were recorded on a Shimadzu RF-5301PC spectrofluorophotometer in the temperature range of 4−45 °C, and the sample was allowed to equilibrate for 12 min at each temperature before the measurements were taken. Excitation spectra were monitored at λ_{em} = 373 nm. Slit widths for both excitation and emission sides were maintained at 3.0 nm. Sample solutions were prepared by dissolving a predetermined amount of bis(adamantyl)-terminated PPGs (guest polymers) and corresponding amount of β-CD-core star polymer (host polymer) in an aqueous pyrene solution (1 mL), and the solutions were allowed to stand for 1 day for equilibration at 4 °C.

The concentration of the 1:1 host−guest mixtures was fixed at 2.0 mg/mL, and the concentration of pyrene was kept at 6.0×10^{-7} M.

Micelle Size Measurements. Measurements of micelle size were performed on the host−guest solutions using a Zetasizer Nano ZS (Malvern Instruments, Southborough, MA) with a laser light wavelength of 633 nm at a 173° scattering angle. The micelle size measurement was performed in the temperature range of 3−45 °C, and the sample was allowed to equilibrate for 12 min at each temperature before the measurements were taken. The convolution of the measured correlation curve to an intensity size distribution was accomplished using a non-negative least-squares algorithm. The decay rate distributions were transformed to an apparent diffusion coefficient (D). From the diffusion coefficient, the apparent hydrodynamic size of the micelles can be obtained by the Stokes−Einstein equation. The Z-average hydrodynamic diameters of the particles were given by the instrument. The Z-average size is the intensity-weighted mean diameter derived from a cumulant or single-exponential fit of the intensity autocorrelation function.

Transmission Electron Microscopy (*TEM*). The samples for TEM were prepared by directly depositing a drop (ca. 5 μL) of 1:1 host−guest solution (2.0 mg/mL, prepared at 14 or 20 °C) containing 0.1 wt % phosphotungstic acid (PTA) onto copper grids, which were coated in advance with supportive Formvar films and carbon (Agar Scientific). The samples were kept in a dry cabinet for 12 h for drying at 14 or 20 °C before they were imaged on a JEOL JEM-2010F FasTEM field emission transmission electron microscope operated at 100 kV.

Atomic Force Microscopy (*AFM*). The AFM imaging was performed in tapping mode using the Dimension 3100 model with Nanoscope IIIa controller (Veeco, Santa Barbara, CA). Commercially available standard silicon probes with spring constant of 40 N/m and a tip radius of 7 nm (PPP-NCH, Nanosensors, Switzerland) was used for imaging. The images were processed and analyzed using the Nanoscope software v5.30r3 (Veeco, Santa Barbara, CA). The sample preparation was similar to that for TEM, but silicon was used as substrate. The silicon substrate was washed with absolute ethanol and dried with nitrogen at room temperature.

Acknowledgment. This work was jointly supported by MINDEF-NUS Joint Applied Cooperation Program (MINDEF/NUS/JPP/10/02), Singapore Ministry of Education Academic Research Fund Tier 2 Grant (R-397-000-031-112), Incentive Funding from Faculty of Engineering, National University of Singapore (R-397-000-031-731), and Institute of Materials Research and Engineering (IMRE), A*STAR (Agency for Science, Technology and Research), Singapore.

Supporting Information Available: A table of selected characterization data for adamantyl-containing PPGs and staring PPGs and figures showing the turbidity variations with temperature for a series of host−guest mixtures with PPG-4K-$(Ad)_2$ and PPG-400-$(Ad)_2$ as guest polymer, respectively. This material is available free of charge via the Internet at http://pubs.acs.org.

References and Notes

(1) Kakizawa, Y.; Kataoka, K. *Adv. Drug Delivery Rev.* **2002**, *54*, 203–222.
(2) Rosler, A.; Vandermeulen, G. W. M.; Klok, H. A. *Adv. Drug Delivery Rev.* **2001**, *53*, 95–108.
(3) Kataoka, K.; Harada, A.; Nagasaki, Y. *Adv. Drug Delivery Rev.* **2001**, *47*, 113–131.
(4) Guo, M. Y.; Jiang, M. *Soft Matter* **2009**, *5*, 495–500.
(5) Chen, D. Y.; Jiang, M. *Acc. Chem. Res.* **2005**, *38*, 494–502.
(6) Wang, J.; Jiang, M. *J. Am. Chem. Soc.* **2006**, *128*, 3703–3708.
(7) Zeng, J.; Shi, K.; Zhang, Y.; Sun, X.; Zhang, B. *Chem. Commun.* **2008**, 3753–3755.
(8) Moughton, A. O.; O'Reilly, R. K. *J. Am. Chem. Soc.* **2008**, *130*, 8714–8725.
(9) Szejtli, J. *Chem. Rev.* **1998**, *98*, 1743–1753.
(10) Wenz, G.; Han, B.-H.; Muller, A. *Chem. Rev.* **2006**, *106*, 782–817.
(11) Hapiot, F.; Tilloy, S.; Monflier, E. *Chem. Rev.* **2006**, *106*, 767–781.
(12) Douhal, A. *Chem. Rev.* **2004**, *104*, 1955–1976.
(13) Harada, A. *Acc. Chem. Res.* **2001**, *34*, 456–464.
(14) Uekama, K.; Hirayama, F.; Irie, T. *Chem. Rev.* **1998**, *98*, 2045–2076.
(15) Rekharsky, M. V.; Inoue, Y. *Chem. Rev.* **1998**, *98*, 1875–1918.
(16) Nepogodiev, S. A.; Stoddart, J. F. *Chem. Rev.* **1998**, *98*, 1959–1976.
(17) Davis, M. E.; Brewster, M. E. *Nat. Rev. Drug Discovery* **2004**, *3*, 1023–1035.
(18) Li, J.; Loh, X. J. *Adv. Drug Delivery Rev.* **2008**, *60*, 1000–1017.
(19) Li, J. *Adv. Polym. Sci.* **2009**, *222*, 79–113.
(20) Zhang, Z.-X.; Liu, X.; Xu, F. J.; Loh, X. J.; Kang, E.-T.; Neoh, K.-G.; Li, J. *Macromolecules* **2008**, *41*, 5967–5970.
(21) Schild, H. G. *Prog. Polym. Sci.* **1992**, *17*, 163–249.
(22) Bromberg, L. E.; Ron, E. S. *Adv. Drug Delivery Rev.* **1998**, *31*, 197–221.
(23) Chaterji, S.; Kwon, I. K.; Park, K. *Prog. Polym. Sci.* **2007**, *32*, 1083–1122.
(24) Chilkoti, A.; Dreher, M. R.; Meyer, D. E.; Raucher, D. *Adv. Drug Delivery Rev.* **2002**, *54*, 613–630.
(25) Da Silva, R. M. P.; Mano, J. F.; Reis, R. L. *Trends Biotechnol.* **2007**, *25*, 577–583.
(26) Gil, E. S.; Hudson, S. A. *Prog. Polym. Sci.* **2004**, *29*, 1173–1222.
(27) Hoffman, A. S.; Stayton, P. S. *Prog. Polym. Sci.* **2007**, *32*, 922–932.
(28) Hou, Q. P.; Bae, Y. H. *Adv. Drug Delivery Rev.* **1999**, *35*, 271–287.
(29) Jeong, B.; Kim, S. W.; Bae, Y. H. *Adv. Drug Delivery Rev.* **2002**, *54*, 37–51.
(30) Kikuchi, A.; Okano, T. *Adv. Drug Delivery Rev.* **2002**, *54*, 53–77.
(31) Kokufuta, E. *Adv. Polym. Sci.* **1993**, *110*, 157–177.
(32) Rzaev, Z. M. O.; Dincer, S.; Piskin, E. *Prog. Polym. Sci.* **2007**, *32*, 534–595.
(33) Schmaljohann, D. *Adv. Drug Delivery Rev.* **2006**, *58*, 1655–1670.
(34) Pintauer, T.; Matyjaszewski, K. *Coord. Chem. Rev.* **2005**, *249*, 1155–1184.
(35) Masci, G.; Giacomelli, L.; Crescenzi, V. *Macromol. Rapid Commun.* **2004**, *25*, 559–564.
(36) Crutchfield, C. A.; Harris, D. J. *Magn. Reson. Chem.* **2007**, *45*, 463–468.
(37) Postma, A.; Davis, T. P.; Donovan, A. R.; Li, G. X.; Moad, G.; Mulder, R.; O'Shea, M. S. *Polymer* **2006**, *47*, 1899–1911.
(38) Hwang, M. J.; Joo, M. K.; Choi, B. G.; Park, M. H.; Hamley, I. W.; Jeong, B. *Macromol. Rapid Commun.* **2010**, *31*, 2064–2069.
(39) Li, J.; He, W. D.; Han, S. C.; Sun, X. L.; Li, L. Y.; Zhang, B. Y. *J. Polym. Sci., Part A: Polym. Chem.* **2009**, *47*, 786–796.
(40) Stoica, F.; Alexander, C.; Tirelli, N.; Miller, A. F.; Saiani, A. *Chem. Commun.* **2008**, 4433–4435.
(41) Kotsuchibashi, Y.; Kuboshima, Y.; Yamamoto, K.; Aoyagi, T. *J. Polym. Sci., Part A: Polym. Chem.* **2008**, *46*, 6142–6150.
(42) Dai, F. Y.; Wang, P. F.; Wang, Y.; Tang, L.; Yang, J. H.; Liu, W. G.; Li, H. X.; Wang, G. C. *Polymer* **2008**, *49*, 5322–5328.
(43) Xu, J.; Luo, S. Z.; Shi, W. F.; Liu, S. Y. *Langmuir* **2006**, *22*, 989–997.
(44) Wu, K.; Shi, L. Q.; Zhang, W. Q.; An, Y. L.; Zhu, X. X. *J. Appl. Polym. Sci.* **2006**, *102*, 3144–3148.
(45) Loh, X. J.; Zhang, Z. X.; Wu, Y. L.; Lee, T. S.; Li, J. *Macromolecules* **2009**, *42*, 194–202.
(46) Zhao, X. L.; Liu, W. G.; Chen, D. Y.; Lin, X. Z.; Lu, W. W. *Macromol. Chem. Phys.* **2007**, *208*, 1773–1781.
(47) Xia, Y.; Burke, N. A. D.; Stöver, H. D. H. *Macromolecules* **2006**, *39*, 2275–2283.
(48) Cheng, C.; Schmidt, M.; Zhang, A.; Schlüter, A. D. *Macromolecules* **2007**, *40*, 220–227.
(49) Qin, S. H.; Geng, Y.; Discher, D. E.; Yang, S. *Adv. Mater.* **2006**, *18*, 2905–2909.
(50) Jeong, B.; Windisch, C. F.; Park, M. J.; Sohn, Y. S.; Gutowska, A.; Char, K. *J. Phys. Chem. B* **2003**, *107*, 10032–10039.
(51) Lee, B. H.; Lee, Y. M.; Sohn, Y. S.; Song, S. C. *Macromolecules* **2002**, *35*, 3876–3879.
(52) Jeong, B.; Bae, Y. H.; Kim, S. W. *Macromolecules* **1999**, *32*, 7064–7069.
(53) Jeong, B.; Bae, Y. H.; Kim, S. W. *Colloids Surf., B* **1999**, *16*, 185–193.

(54) Astafieva, I.; Zhong, X. F.; Eisenberg, A. *Macromolecules* **1993**, *26*, 7339–7352.
(55) Wilhelm, M.; Zhao, C. L.; Wang, Y. C.; Xu, R. L.; Winnik, M. A.; Mura, J. L.; Riess, G.; Croucher, M. D. *Macromolecules* **1991**, *24*, 1033–1040.
(56) Li, J.; Ni, X. P.; Li, X.; Tan, N. K.; Lim, C. T.; Ramakrishna, S.; Leong, K. W. *Langmuir* **2005**, *21*, 8681–8685.
(57) Li, X.; Mya, K. Y.; Ni, X. P.; He, C. B.; Leong, K. W.; Li, J. *J. Phys. Chem. B* **2006**, *110*, 5920–5926.
(58) Loh, X. J.; Wu, Y. L.; Seow, W. T. J.; Norimzan, M. N. I.; Zhang, Z. X.; Xu, F.; Kang, E. T.; Neoh, K. G.; Li, J. *Polymer* **2008**, *49*, 5084–5094.
(59) Britovsek, G. J. P.; England, J.; White, A. J. P. *Inorg. Chem.* **2005**, *44*, 8125–8134.